Aerodynamic Performances of Propellers with Parametric Considerations on the Optimal Design

S. D'Angelo, F. Berardi, E. Minisci

Department of Aeronautical and Space Engineering

Politecnico di Torino, Turin - Italy

ABSTRACT

In this paper two numerical procedures are presented: the first algorithm allows for the determination of the geometric characteristics of the maximum efficiency propeller for a given operative condition and profile distribution along the blade; the output of this numerical procedure is the chord distribution and twist angle of the blade, together with its efficiency and its torque and thrust coefficients for the prescribed operative condition. The aerodynamic characteristics of the optimum propeller when operating in a condition different from the design one are obtained by a second algorithm that allows for the evaluation of the efficiency, the thrust and torque coefficients of a propeller of known geometry, when the blade pitch and operative condition are varied.

In the paper the formulation used for deriving the geometry of the optimum propeller and determining its performances when operating off-design is described in detail. The results obtained from the proposed propeller model have been validated by comparison with experimental data.

Nomenclature

b non dimensional blade section chord, $b=l/R$

c sound speed

c_d airfoil drag coefficient

c_l airfoil lift coefficient

$\boldsymbol{D}$ drag

E aerodynamic efficiency

$\boldsymbol{F_A}$ total aerodynamic force

k_P Prandtl correction factor

K Lagrange factor (constant)

l blade section chord

$\boldsymbol{L}$ lift

$\boldsymbol{M}$ engine torque

Ma free stream Mach number, $Ma=V/c$

Ma_ξ local Mach number at station ξ, $Ma_\xi=V_E/c$

n blade number

P shaft power

r coordinate along blade span

R propeller radius

Re free stream Reynolds number, $Re=R*V*\rho/\mu$

Re_ξ local Reynolds number at station ξ, $Re=l*V_E*\rho/\mu$

$\boldsymbol{T}$ thrust

$\boldsymbol{u_D}$ induced velocity in the plane of the propeller

$\boldsymbol{V}$ forward speed

$\boldsymbol{V_A}$ apparent velocity, $V_A=(V^2+(\Omega r)^2)^{1/2}$

$\boldsymbol{V_E}$ actual velocity of flow approaching the airfoil

$\hat{V}_E$ non dimensional actual velocity, $\hat{V}_E=V_E/V$

α actual airfoil angle of attack

α_A apparent airfoil angle of attack

α_{Emax} angle of attack for maximum airfoil efficiency

α_i induced incidence

α_{tw} twist angle

γ advance ratio

Γ circulation

δ angle between actual velocity and propeller plane

δ_A angle between apparent velocity and propeller plane

η efficiency

θ blade section pitch angle relative to propeller plane, $\theta(\xi)=\alpha_{tw}(\xi)+\theta_0$

θ_0 collective pitch, $\theta_0=\theta(\xi=0.75)$

μ air viscosity

ξ non dimensional coordinate along the blade

ρ air density

τ thrust coefficient

χ torque coefficient

ω angular component of induced velocity in the propeller plane

Ω propeller angular velocity

INTRODUCTION

The numerical procedure proposed in the present paper requires the a priori knowledge of the aerodynamic characteristics of the airfoils used for the propeller. This can be obtained from an experimental or computational data-base.

It is not always possible to obtain detailed data-bases that take into consideration both Reynolds and Mach number effects in such a wide range as that encountered at different sections of an aeronautical propeller blade. Linear interpolation and extrapolation between experimental data is used in order to

take into consideration Reynolds number variation, while semi empirical corrections are implemented for taking into consideration compressibility effects.

The propeller performance determined by a simplified numerical procedure compare well with the experimental results obtained from wind-tunnel tests, as far as the section at 0.75 of blade span is operating below stall angle and below drag-divergence Mach number in the considered condition.

In what follows, the classical aerodynamic propeller theory is discussed. The formulation is oriented towards the implementation of a numerical algorithm for the determination of the propeller of maximum efficiency for a given operating condition.

After a detailed discussion of the aerodynamic theory of propellers, the experimental database of airfoil characteristics used in the evaluation of the optimum blade is presented and a comparison between experimental data and numerical results for the given airfoil is discussed for validating the proposed algorithm.

A parametric study of the optimum blade shape at different operating points is presented, so as to derive some general considerations on the geometry of the maximum efficiency propeller. These general principles can be useful in defining proper initial solutions when more sophisticated optimization tools are used, with merit functions different from the aerodynamic efficiency or even in the case of multi-objective optimization.

The same formulation used for the optimization routine is implemented in a second numerical algorithm for the evaluation of the aerodynamic characteristics of a given propeller in any operating condition, in terms of blade pitch, θ, and advance ratio, γ. The values of thrust coefficient, torque coefficient and efficiency are obtained, i.e. $\tau(\theta, \gamma)$, $\chi(\theta, \gamma)$, and $\eta(\theta, \gamma)$.

This routine is validated comparing its results with available experimental data. The accuracy of the numerical prediction seems to be satisfactory from an engineering standpoint. Moreover the computational effort required by the proposed algorithm is very limited and this make it suitable for its implementation in different optimization procedures, single objective or multi-objective, deterministic or non-deterministic.

1 From aerodynamic propeller theory to propeller design.

In this paper we will consider propeller generating thrust in an axial flow. The blade has variable chord and twist angle but the feathering axis is assumed rectilinear and lying in a plane during the revolution.

The aerodynamic theory adopted is based on classical results [1], [2], obtained from the integration of vortex theory, wing theory and momentum theory.

When vortex theory is adopted, propeller thrust and torque are expressed as a function of circulation along the blade. Thrust distribution of minimum energy dissipation is obtained by a variational approach, adopting Prandtl simplified approach [3].

If wing theory is chosen for representing the aerodynamic behavior of the blade, thrust and torque are obtained from integration of elementary lift and drag contribution acting on an infinitesimal blade element. The induced velocity is evaluated locally combining results from wing theory and momentum conservation principle.

1.1 Vortex theory

Figure 1 represent a generic blade element. The meaning of the symbols used in the following pages can be found in the Nomenclature and is represented in the same figure.

The actual velocity of the flow past a given section, $\boldsymbol{V_E}$, is given by the vector sum of the apparent velocity, $\boldsymbol{V_A}$, and the induced velocity increment at the considered section $\boldsymbol{u_D}$. $\boldsymbol{V_A}$ is given by the sum of forward speed $\boldsymbol{V}$ and rotational speed of the section $\boldsymbol{\Omega} r$.

When a blade element dr at position r along the blade span is considered, the circulation $\Gamma(r)$ can be expressed according to Prandtl approximation as:

$$\Gamma = \frac{2\pi r}{n} 2\omega r \, k_P \tag{1}$$

$$k_P = \frac{2}{\pi}\arccos\left\{\exp\left[-\frac{n}{2}\left(1-\frac{r}{R}\right)\sqrt{1+\left(\frac{\Omega R}{V}\right)^2}\right]\right\} \tag{2}$$

Thrust, torque, and power dissipated by the propeller are obtained integrating the elementary components along a single blade and multiplying the result by the number of blades.

On a given blade element, the aerodynamic force $d\boldsymbol{F_A}$, thrust $d\boldsymbol{T}$, torque $d\boldsymbol{M}$ and dissipated energy per second dP_d are given respectively by:

$$dF_A = \rho\, \Gamma V_E\, dr \tag{3}$$

$$dT = \rho\, \Gamma V_E \cos\delta\, dr \tag{4}$$

$$dM = \rho\, \Gamma V_E \sin\delta\, r\, dr \tag{5}$$

$$dP_d = \rho\, \Gamma V_E \left(\Omega r \sin\delta - V\cos\delta\right) dr \tag{6}$$

Calculus of variations allows for the determination of the optimal circulation distribution $\Gamma(r)$ that minimizes the energy loss for a given thrust $\boldsymbol{T}$.

Letting $-KV$ be the Lagrange factor, the derivative of the linear combination of thrust and power loss is equated to zero. The resulting equation is solved with respect to the circulation Γ, and the condition for minimum power loss is obtained:

$$\tan\delta = \frac{V}{\Omega r}\left(1+K\right) \tag{7}$$

The circulation distribution, the actual velocity and induced velocity for the section at coordinate r from the propeller axis are then expressed by:

$$\Gamma = \frac{4\pi r}{n} KV \cos\delta \sin\delta\, k_P \tag{8}$$

$$V_E = \frac{\Omega r - \omega r}{\cos\delta} = V\frac{1 + K\cos^2\delta}{\sin\delta} \tag{9}$$

$$\tan\alpha_i = \frac{u_D}{V_E} = \frac{K\sin\delta\cos\delta}{1 + K\cos^2\delta} \tag{10}$$

Given *n*, *T*, *V*, Ω, and *R*, the Lagrange multiplier can be obtained in two different ways:

a) by numerical solution of the implicit function:

$$\frac{T}{\rho\, 4\pi V^2} = \int_0^R \left(K_1 + K_1^{\,2}\right) k_P r dr \tag{11}$$

where

$$K_1 = \frac{K}{1 + \left(\frac{V}{\Omega r}\right)^2 (1 + K)^2} \tag{12}$$

b) by a simplified formulation obtained neglecting K^2 with respect to the first order term as far as $|K| << 1$, so that:

$$K = \frac{T}{F_1 \rho\, 4\pi V^2} \tag{13}$$

where

$$F_1 = \int_0^R \frac{(\Omega r)^2 k_P r}{V^2 + (\Omega r)^2}\, dr \tag{14}$$

1.2 Wing theory

As stated in the introduction, the wing theory allows for the evaluation of thrust and torque generated by a propeller in a given operating condition by integrating the elementary aerodynamic actions acting on an infinitesimal portion *dr* of the blade.

In this case elementary thrust and torque are expressed as:

$$dT = \frac{1}{2}\rho V_E^2 \left(c_l \cos\delta - c_d \sin\delta\right) l \, dr \tag{15}$$

$$dM = \frac{1}{2}\rho V_E^2 \left(c_l \sin\delta + c_d \cos\delta\right) l \, r \, dr \tag{16}$$

The actual velocity and the induced incidence are obtained equating the expression for the propeller thrust derived from vortex theory and that obtained by wing theory. The resulting expressions are:

$$V_E = V_A \cos\alpha_i = V\sqrt{1+\left(\frac{\Omega r}{V}\right)^2}\cos\alpha_i \tag{17}$$

$$\tan\alpha_i = \frac{nl}{8\pi r k_P}\frac{c_l \cos\delta - c_d \sin\delta}{\sin\delta \ \cos\delta} \tag{18}$$

2 Non-dimensional coefficient and independent parameters

The advance ratio γ, the thrust coefficient τ, the torque coefficient χ, and the propeller efficiency η are defined as follows:

$$\gamma = \frac{V}{\Omega R} \tag{19}$$

$$\tau = \frac{T}{\rho \Omega^2 R^4} \tag{20}$$

$$\chi = \frac{M}{\rho \Omega^2 R^5} \tag{21}$$

$$\eta = \frac{TV}{P} = \frac{\tau\gamma}{\chi} \tag{22}$$

Thrust and torque coefficients can be expressed as a function of 6 independent parameters, i.e.:

$$\tau = \tau(V, R, \Omega, \rho, \mu, c) \tag{23}$$

$$\chi = \chi(V, R, \Omega, \rho, \mu, c) \tag{24}$$

If we apply the theorem of Buckingam, we obtain the following relations in terms of non-dimensional parameters:

$$\tau = \tau\left(\frac{V}{\Omega R}, \frac{\rho VR}{\mu}, \frac{V}{c}\right) = \tau(\gamma, Re, Ma) \tag{25}$$

$$\chi = \chi\left(\frac{V}{\Omega R}, \frac{\rho VR}{\mu}, \frac{V}{c}\right) = \chi(\gamma, Re, Ma) \tag{26}$$

where *Ma* is the Mach number of the undisturbed flow upstream the propeller, while *Re* is the Reynolds number, the reference length being the propeller radius *R*.

We will assume that the influence of *Re* and *Ma* on τ e χ is due only to their effect on the aerodynamic coefficients c_l e c_d of each blade section, i.e. on the aerodynamic characteristics of each airfoil.

Finally we will introduce also the following non-dimensional quantities:

$$\xi = \frac{r}{R} \tag{27}$$

$$b = \frac{l}{R} \tag{28}$$

$$\hat{V}_E = \frac{V_E}{V} \tag{29}$$

$$Re_\xi = \frac{V_E l}{\nu} = \hat{V}_E b \cdot Re \tag{30}$$

$$Ma_\xi = \frac{V_E}{c} = \hat{V}_E \cdot Ma \tag{31}$$

where ξ is a non-dimensional coordinate along the blade radius, *b* is the blade section non-dimensional chord, $\hat{V}_E$ is the non-dimensional actual velocity past the considered blade section, Re_ξ and Ma_ξ are the local Reynolds and Mach number, respectively.

3 Aerodynamic database

The evaluation of the aerodynamic performance of a propeller requires the detailed knowledge of characteristic of the airfoil used for the blades. The aerodynamic database should provide the values of airfoil drag and lift coefficients as a function of angle of attack and Reynolds number.

Usually different airfoils are used along the blade, but aerodynamic characteristics are available for only few of them. In this case it is assumed that intermediate sections between known profiles are characterized by an "intermediate" aerodynamic behaviour, i.e. lift and drag coefficients are obtained by a proper linear combination that weights the airfoil characteristics as a function of the relative distance from the profiles with known characteristics. If *x* is a local non dimensional coordinate between the known sections, lift and drag coefficient for non-compressible flow will be expressed as:

$$c_{li} = c_{li}\left(\alpha, Re_\chi, x\right) \tag{32}$$

$$c_{di} = c_{di}\left(\alpha, Re_\chi, x\right) \tag{33}$$

In order to obtain significant results from the interpolation, it is necessary to consider the effects of Reynolds number on the aerodynamic coefficients, as far as Re_x experiences a significant variation when different sections are considered.

3.1 Compressibility correction

Compressibility effects can have a sizeable influence on the values of lift and drag coefficients.

The local Mach number along an aeronautical propeller blade can vary in such a wide range that this effects cannot be neglected without an unacceptable loss of accuracy. If aerodynamic data exhaustively include compressibility effects it is possible to interpolate aerodynamic data with respect to Mach number in the same way as it is done for Reynolds number. When the available data are limited to low Mach number, a semi-empirical factor is derived so as to provide the necessary correction for c_l and c_d due to compressibility effects from their values for the case of non compressible flow

The correction factor used in the present paper was originally derived for symmetrical airfoils with relative thickness t = 0.21, for $Ma < 0{,}9$ and $-25° \leq \alpha \leq 25°$, but it is reasonable to extend the use of this correction to airfoils with moderate camber and higher values of relative thickness.

The determination of the correction factor is based on:

- the determination of the local critical Mach number
- the determination of the local drag-rise Mach number
- the correction of the aerodynamic coefficients

The critical Mach number is related to the minimum pressure coefficient acting on the airfoil in a non-compressible flow by ([4], [5]):

$$c_{pi,min} = \frac{2\sqrt{1-Ma_{cr}^2}}{\frac{1.4Ma_{cr}^2}{\left(\frac{1+0.2Ma_{cr}^2}{1.2}\right)^{3.5}-1}+\sqrt{1-Ma_{cr}^2}-1} \tag{34}$$

Reference 6 provides the value of the minimum pressure coefficient at zero lift incidence, $c_{pi,min0}$, for several airfoil. From this data it is possible to express $c_{pi,min0}$ for the 4 digit NACA profiles as a function of the relative thickness as follows:

$$c_{pi,min0} = -4{,}764t^2 - 2{,}266t - 0{,}070 \tag{35}$$

Another relation between minimum pressure coefficient and lift coefficient in incompressible flow and relative thickness *t*, is discussed in Ref. 7:

$$c_{pi,min} = -\frac{c_{li}^2}{t} \tag{36}$$

The results obtained from this latter approach show a poor agreement with experimental data, as it is clearly visible in Fig. 2.

A better representation is obtained by adding to $c_{pi,min0}$ a contribution proportional to c_{li}^2/t, with a coefficient *a* smaller than unity. Comparison with the same experimental data provided for *a* a value of 0.75, so that we can express $c_{pi,min}$ as:

$$c_{pi,min} = c_{pi,min0} - a\frac{c_{li}^2}{t} = -4{,}764t^2 - 2{,}266t - 0{,}070 - 0{,}75\frac{c_{li}^2}{t} \tag{37}$$

The value of the critical Mach number is obtained solving the following equation:

$$-4{,}764t^2 - 2{,}266t - 0{,}070 - 0{,}75\frac{c_{li}^2}{t} = \frac{2\sqrt{1-Ma_{cr}^2}}{\dfrac{1.4Ma_{cr}^2}{\left(\dfrac{1+0.2Ma_{cr}^2}{1.2}\right)^{3.5}-1} + \sqrt{1-Ma_{cr}^2} - 1} \tag{38}$$

In most cases Ma_{cr} indicates a threshold beyond which compressibility effects on aerodynamic performance can no longer be neglected, even if there are no immediate consequences. But when the ratio Ma/Ma_{cr} is greater than a value between 1.04 and 1.20, drag increases dramatically.

The value of Ma for which $dc_d / dMa = 0.1$ is the drag rise Mach number, Ma_{DR}, and indicates a limit beyond which airfoil aerodynamic performance degrades seriously.

From the experimental data reported in Ref. [8] and [6], a relation between Ma_{DR} and Ma_{cr} is derived, where the lift coefficient in incompressible flow appears as a parameter:

$$Ma_{DR} = Ma_{cr}\left(1{,}04 + 0{,}4c_{li} - 0{,}25c_{li}^2\right) \tag{39}$$

When $Ma < Ma_{DR}$, the lift coefficient increases with Mach number, for the same incidence.

The lift coefficient in compressible flow, c_{lc}, is obtained according to Kaplan relation (that is a modified version of Prandtl-Glauert correction factor):

$$\frac{c_{lc}}{c_{li}} = \beta_{PG} + \frac{t}{1+t}\left[\beta_{PG}\left(\beta_{PG} - 1\right) + \frac{1}{4}\left(\kappa + 1\right)\left(\beta_{PG}{}^2 - 1\right)^2\right] = \beta_{KA} \tag{40}$$

$$\frac{c_{lc}}{c_{li}} = \frac{1}{\sqrt{1 - Ma^2}} = \beta_{PG} \tag{41}$$

For $Ma > Ma_{DR}$, lift coefficient starts to decrease with Mach number, with a minimum for Ma ≅ 0.9. In this case the correction factor is:

$$c_{lc} = c_{li}\beta_{KA}\frac{1 - Ma^2}{1 - Ma_{DR}^2} \tag{42}$$

The drag coefficient c_d does not depend on Mach number below Ma_{DR}, but, for $Ma > Ma_{DR}$, energy loss caused by the shock wave is responsible of a sharp increase in aerodynamic drag. The drag coefficient is evaluated adding to its value for non-compressible flow C_{di} a contribution due to wave drag, according to [9], [10]:

$$c_{dc} = c_{di} + 1{,}1\left(\frac{Ma - Ma_{DR}}{1 - Ma_{DR}}\right)^3 \tag{43}$$

A comparison between experimental data (in Ref. [8]) and results obtained according to the corrections of non-compressible coefficients is reported in Figs. 3 and 4. It is evident that we have good agreement for values of the angle of attack below stall. As a final consideration on this correction procedure for compressibility effects, we underline that the results are accurate for symmetrical profiles, with thickness ratio less than 0.15 and for Mach number between 0.3 and 0.9, in the linear range of the lift curve. The simplicity of the procedure allows for a reduced computational effort.

4 Characteristics of an *n*-blades propeller of radius *R*

The feathering axis of the blade, represented by a non-dimensional coordinate ξ in the interval [0,1], is divided into m_ξ elements, thus defining m_ξ +1 sections. The active portion of the blade begins at ξ_{min} and n_ξ is the number of sections with $\xi \geq \xi_{min}$. If n_p sections airfoils of known characteristics are used, the generic airfoil at coordinate ξ along the blade will be identified by the distance x from the closest airfoil i_p on the hub side and the distance 1 - x from the closest airfoil i_p +1 on the tip side.

Our problem can be stated as follows: evaluate thrust, torque and efficiency of a propeller with n blades of known geometry (radius R, chord distribution, twist angle), from the aerodynamic characteristics of the airfoil used, for given operating conditions (forward speed, V, angular velocity, Ω, altitude and blade pitch, the latter being defined as the pitch angle of the section at 0.75·R).

For any blade section the local aerodynamic characteristics are evaluated according to wing theory. It is thus necessary to calculate actual velocity, its angle with respect to the propeller disk and the aerodynamic coefficients of the sections as a function of the induced incidence.

In non-dimensional terms the thrust and torque coefficients and the propeller efficiency are evaluated as a function of blade number n, $b(\xi)$, α_{tw}, airfoil characteristics, γ, Re, Ma, θ_0.

The software input is divided into two sets of parameters, the first one for describing the propeller operating point, the second for the propeller aerodynamic characteristics and discretization parameters:

- blade number, n
- number of discretization intervals, n_ξ

- number of airfoils with known aerodynamic characteristics, n_p
- aerodynamic characteristics of the known airfoils
- for each value of ξ_j , j = 1, 2, …, n_ξ, the values of b, α_{tw}, i_p (index of the closest known airfoil on the hub side, i.e. airfoil 1), $i_p + 1$ (index of the closest known airfoil on the tip side, i.e. airfoil 2), the value of x, non-dimensional distance from airfoil 1, i.e. $x = (\xi_j - \xi_{ip})/(\xi_{ip+1} - \xi_{ip})$.

For every section the evaluation of the aerodynamic coefficients is carried out according to the procedure outlined in the previous paragraph. Given the values of γ, Re, Ma, θ, n, b, α_{tw} and profile distribution along the blade, the values of δ, α, and α_i are determined by iteration for α_i. Starting from the relations:

$$\hat{V}_E = \sqrt{1+\left(\frac{\xi}{\gamma}\right)^2}\cos\alpha_i \tag{44}$$

$$\delta = \arctan\left(\frac{\gamma}{\xi}\right) + \alpha_i \tag{45}$$

$$\alpha = \theta_0 + \alpha_{tw} - \delta \tag{46}$$

$$Re_\xi = \hat{V}_E b \cdot Re \tag{47}$$

$$Ma_\xi = \hat{V}_E \cdot Ma \tag{48}$$

the local aerodynamic coefficients are evaluated:

$$c_l = c_l\left(\alpha, Re_\xi, Ma_\xi\right) \tag{49}$$

$$c_d = c_d\left(\alpha, Re_\xi, Ma_\xi\right) \tag{50}$$

$$k_P = \frac{2}{\pi}\arccos\left\{\exp\left[-\frac{n}{2}(1-\xi)\sqrt{1+\frac{1}{\gamma^2}}\right]\right\} \tag{51}$$

$$\tan\alpha_i = \frac{nb}{8\pi\xi\, k_P}\left(\frac{c_l}{\sin\delta} - \frac{c_d}{\cos\delta}\right) \tag{52}$$

Once convergence on α_i is reached, the local increments for thrust and torque coefficients are expressed as follows:

$$d\tau = \frac{\gamma^2}{2}\hat{V}_E^2\left(c_l\cos\delta - c_d\sin\delta\right)b\,d\xi \tag{53}$$

$$d\chi = \frac{\gamma^2}{2}\hat{V}_E^2\left(c_l\sin\delta + c_d\cos\delta\right)b\,\xi\,d\xi \tag{54}$$

Finally the values of $d\tau$ and $d\chi$ are integrated along the blade span, giving:

$$\tau = n\int_{\xi_{\min}}^{1} d\tau \tag{55}$$

$$\chi = n\int_{\xi_{\min}}^{1} d\chi \tag{56}$$

$$\eta = \frac{\tau\gamma}{\chi} \tag{57}$$

4.1 Comparison with experimental data

A comparison between numerical results and experimental data reported in Ref. 11 is presented in Figs. 5, 6 and 7 to validate the proposed algorithm. The aerodynamic characteristics of the airfoils of the NACA 44XX series used for the propeller analyzed in Ref. 11 were obtained from Refs. 12 and 6. The values of τ, χ and η are reported in Figs. 5, 6 and 7, respectively, as a function of the advance ratio γ.

The agreement between our method and experimental results appears satisfactory when the representative section local Mach number is below Ma_{DR} and is angle of attack is below stall. For

higher values of local velocity or blade pitch angle the empirical corrections are no longer sufficient for obtaining an accurate representation of the complex physical phenomena around a consistent portion of the blade.

In particular, the plots show an overoptimistic prediction of the propeller performance for high values of the blade pitch angle.

5 Design of the maximum efficiency propeller

In this paragraph a numerical procedure for the determination of twist angle and chord distribution as a function of the distance *r* from the hub for an *n*-blade propeller of radius *R* is presented. The optimum propeller will minimizes the energy loss for providing a required thrust *T*, given the operating point in terms of forward speed, propeller angular velocity and altitude.

The maximum efficiency of the propeller will be obtained if all the airfoils along the blade span are at their maximum efficiency angle of attack. For each section, the angle of attack for maximum efficiency is determined, as a function of local Reynolds and Mach number. An iterative procedure is necessary for determining the value of the airfoil chord for a given section.

The resulting chord and twist angle distributions along the blade will depend on 4 independent parameters, thrust coefficient τ, advance ratio γ, Reynolds and Mach numbers, *Re*, *Ma*. A parametric study of the optimum blade shape as a function of these parameters provides interesting results.

The numerical procedure for determining the optimum blade shape, can be summarized as follows.

Again, the input data can be grouped into three sets, a first one for the operating point, τ, γ, *Re* and *Ma*, and a second one, with the propeller characteristics already assigned by the designer:

– blade number, *n*,

– airfoil distribution along the blade,

– aerodynamic characteristics of the airfoil used and the last one, given by the disctretization parameters.

First of all, the Lagrange multiplier *K* is determined:

for every section ξ_i of the discretized blade, where $i = 1, 2, \ldots, n_\xi$, it is:

$$k_P = \frac{2}{K}\arccos\left\{\exp\left[-\frac{n}{2}(1-\xi_i)\sqrt{1+\frac{1}{\gamma^2}}\right]\right\} \tag{58}$$

$$K_1 = \frac{K}{1+\left(\frac{\gamma}{\xi_i}\right)^2(1+K)^2} \tag{59}$$

The equation

$$\frac{\tau}{4\pi\gamma^2} = \int_{\xi_{min}}^{1}\left(K_1 + K_1^{\,2}\right)k_P\xi\, d\xi \tag{60}$$

is then solved numerically by a bisection method.

The distribution of twist angle and profile chord along the blade is determined as follows. The angle δ and the local velocity are given by:

$$\delta = \arctan\left[\frac{\gamma}{\xi_i}(1+K)\right] \tag{61}$$

$$\alpha_i = \arctan\left(\frac{K\sin\delta\cos\delta}{1+K\cos^2\delta}\right) \tag{62}$$

$$\hat{V}_E = \sqrt{1+\left(\frac{\xi_i}{\gamma}\right)^2}\cos\alpha_i \tag{63}$$

For each section ξ_i the following equations are iterated until convergence is reached:

$$Re_\xi = \hat{V}_E b \cdot Re \tag{64}$$

$$Ma_\xi = \hat{V}_E \cdot Ma \tag{65}$$

Then the angle of attach of maximum efficiency is determined:

$$\alpha_{Emax} = \alpha_{Emax}\left(x, Re_{\xi}, Ma_{\xi}\right) \tag{66}$$

where *x* and *1-x* are the relative distance from the nearest known airfoils (see par. 4)

$$b = \frac{8\pi}{n} \frac{\xi_i \, k_P \tan\alpha_i \sin\delta}{c_l(\alpha_{Emax}) - c_d(\alpha_{Emax})\tan\delta} \tag{67}$$

When convergence is reached, the resulting local pitch angle is given by:

$$\theta = \delta + \alpha_{Emax} \tag{68}$$

Then the global characteristics are determined by numerical integration of

$$\tau = \int_{\xi_{min}}^{1} d\tau \tag{69}$$

$$\chi = \int_{\xi_{min}}^{1} d\chi \tag{70}$$

where

$$d\tau = \frac{n\gamma^2}{2} \hat{V}_E^2 \left(c_l \cos\delta - c_d \sin\delta\right) b \, d\xi \tag{71}$$

$$d\chi = \frac{n\gamma^2}{2} \hat{V}_E^2 \left(c_l \sin\delta + c_d \cos\delta\right) b \, \xi \, d\xi \tag{72}$$

The resulting efficiency is

$$\eta = \frac{\tau\gamma}{\chi} \tag{73}$$

At the end of the procedure it is necessary to check whether the assigned blade number *n* is compatible

with the prescribed operating point. In particular, if $b_{max}/R < 0.15$ it is necessary to reduce n for structural reasons, while if $b_{max}/R > 0.24$, increasing n can produce significant improvement in terms of aerodynamic efficiency.

5.1 Parametric analysis of the optimum blade

The geometry of the optimum blade depends on the non-dimensional parameters τ, γ, Re and Ma. A parametric study is presented, limiting, for the sake of simplicity, the analysis to the study of two-bladed propellers with constant airfoil NACA 0012. The characteristics of this airfoil are known with great detail and the compressibility correction is particularly well suited.

The range of variation of the parameters representing the operating point of the propeller are determined taking into consideration 20 single engine airplanes with two blade propellers.

Their characteristics in terms of cruise altitude and airspeed, thrust, diameter and angular velocity have been converted into non-dimensional coefficients. For each of the four parameters, three significant values were determined, a mean value, and a higher and a lower bound.

The optimum propeller was determined for several significant combinations of the 4 parameters.

Finally, the influence of a single parameter was analyzed repeating the design of the optimum shape, letting the parameter vary in the whole admissible range, keeping the other three fixed. It easy to note that the advance ratio have a significant influence on both twist angle and chord distributions (Fig. 8). Increasing γ, the maximum chord section moves towards the blade tip, the propeller solidity decreases and the twist angle is modified in order to reduce the pitch angle at the root of the blade.

The thrust coefficient does not have a significant influence on twist angle and chord distribution, but higher values of τ require propellers with increased solidity (Fig. 9).

Mach number has a great influence on chord distribution, especially in the tip region, where compressibility effects are more significant (Fig. 10). In particular, the chord in the tip region is characterized by large values even for limited increments of Mach number.

Reynolds number does not influence any of the geometrical characteristics of the optimum propeller

for $Re > 3\ 10^6$. Only in the low *Re* region, a decrease in *Re* causes an increase in propeller solidity (Fig. 11).

6 Conclusions

On the basis of Vortex theory and Wing theory two algorithms that can be used to design and numerically test a propeller have been described. The first one supplies the characteristic of the propeller functioning in given conditions, once the blade geometry and the aerodynamic characteristics of the main section profiles are known. Results, compared to experimental data found in literature, show a good agreement in the range of operating points where the propeller is more likely to operate. The second one supplies the blade geometry of the maximum efficiency propeller operating in given conditions and delivering a required thrust level, once the aerodynamic characteristics of the main section profiles are known. Results of the latter algorithm are used to perform a parametric analysis on the shape of the optimum blade.

The tool composed by the implementation of both the algorithms could be helpful in the framework of preliminary design, especially if we consider that much more complex and expensive CFD applications are necessary for obtaining only a minor improvement in the performance of the propeller. For this reason it will be possible to use this tool as a baseline model for several applications, e.g. multi-objective optimization design, multi-objective improvement design, etc.

Other algorithms for propeller design and analysis were developed in the last 20 years, based on the same basic aerodynamic theories ([13] – [15]). The originality of the approach proposed in the present paper lies in the determination of the aerodynamic characteristics of intermediate airfoils by interpolating those of two known airfoils, thus allowing for the development of an easy to use set of algorithms, helpful in the design and analysis of aeronautical propellers, starting from a possibly limited set of experimental airfoil data. Moreover, compressibility corrections can be included in the analysis, even if the available data do not take into account Mach number effects.

REFERENCES

1. Pistolesi, E., *"Aerodinamica"*, Torino, UTET, 1932.
2. Goldstein, *"On the Vortex Theory of Screw Propellers"*, Proceedings of the Royal Society 123, 1929.
3. Prantl, Betz et al., *"Schraubenpropeller mit geringstem Energieverlust"*, Nachrichten d. K. Gesellschaft der Wissenschaften zu Göttingen, 1919.
4. Hilton, W.F., *"High speed aerodynamics"*, New York, Longmans, Green and Co., 1951.
5. Dommash, D.O., Sherby, S.S., Connolly, T.F., *"Airplane aerodynamics"*, New York, Pitman Publishing Corporation, 1967.
6. Abbott, I.H., von Doenhoff, A.E., *"Theory of Wing Sections"*, New York, Dover, 1959.
7. Hoerner, S.F., Borst, H.V., *"Fluid-dynamic lift"*, 2 ed., Brick Town, Hoerner,. 1985.
8. Carpenter, P.J., *"Lift and profile-drag characteristics of an NACA 0012 airfoil section as derived from measured helicopter hovering performance"*, NACA TN 4357, 1958.
9. Hoerner, S.F., *"Fluid-dynamic drag"*, Brick Town, Hoerner, 1958.
10. Martinov, A.K., *"Practical aerodynamics"*, Oxford, Pergamon press, 1965.
11. Biermann, D., Hartman, E. P., *"The aerodynamic characteristics of six full-scale propellers having different airfoil sections"*, NACA Report 650, 1939.
12. Loftin, L.K. Jr., Smith, H.A., *"Aerodynamic characteristics of 15 NACA airfoil sections at seven Reynolds numbers from 0.7×10^6 to 9.0×10^6"*, NACA TN 1945, 1949.
13. Larrabee, E.E., *"Practical Design of Minimum Induced Loss Propellers"*, SAE Preprint 790585, 1979.
14. Eppler, R., Hepperle, M., *"A Procedure for Propeller Design by Inverse Methods"*, published in: G.S. Dulikravich, proceedings of the International Conference on Inverse Design Concepts in Engineering Sciences (ICIDES), Austin TX, October 17-18, 1984.
15. Simonetti, F., Ardito Marretta, R.M., *"A numerical variational approach for rotor-propeller aerodynamics in axial flight"*, Computer Modeling in Engineering & Sciences, Vol. 1, n. 3, 2000.

List of figures

Fig. 1 – Generic blade element at position *r*

Fig. 2 - Minimum pressure coefficient in incompressible flow

Fig. 3 – NACA 0012: Lift coefficient versus angle of attack and Mach number

Fig. 4 – NACA 0012: Drag coefficient versus Mach number and angle of attack

Fig. 5 – Thrust coefficient versus advance ratio and blade pitch angle

Fig. 6 – Torque coefficient versus advance ratio and blade pitch angle

Fig. 7 – Efficiency versus advance ratio and blade pitch angle

Fig. 8 – Advance ratio effects

Fig. 9 – Thrust coefficient effects

Fig. 10 – Mach number effects

Fig. 11 – Reynolds number effects

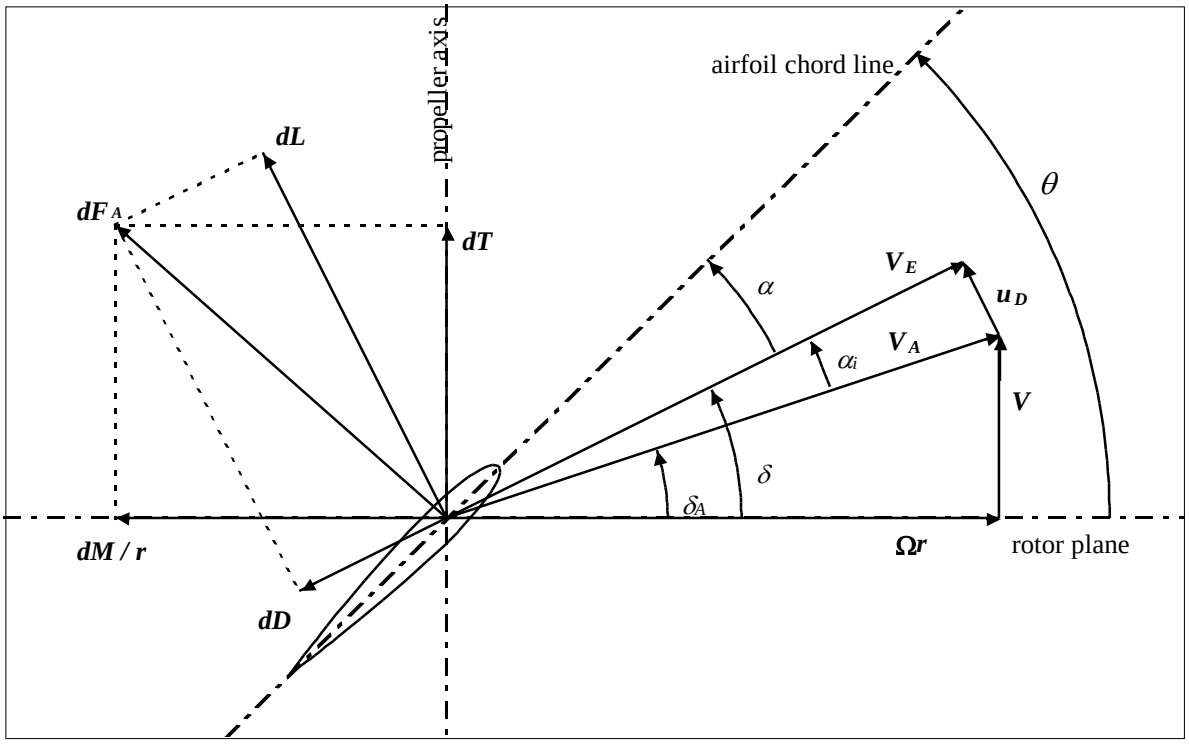

Fig. 1 – Generic blade element at position *r*

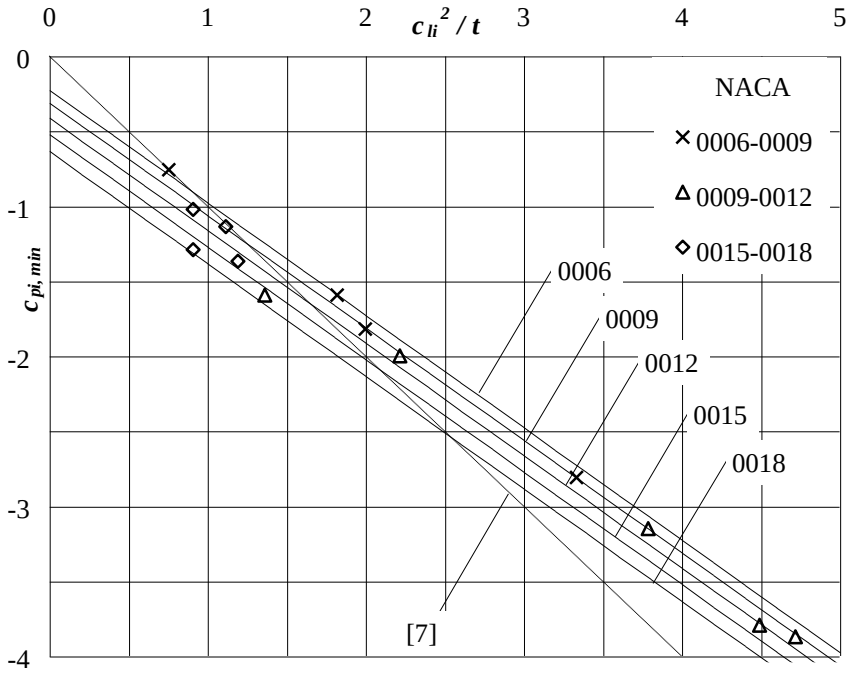

Fig. 2 Minimum pressure coefficient in incompressible flow

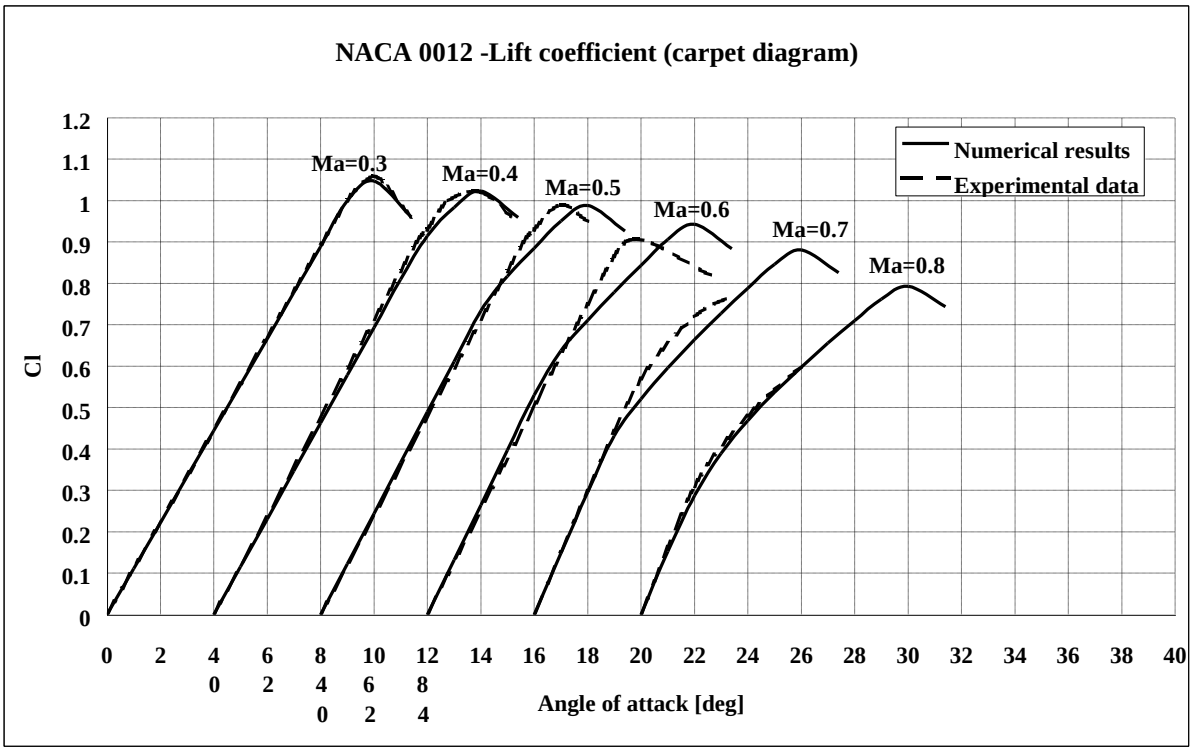

Fig. 3 – NACA 0012: Lift coefficient versus angle of attack and Mach number

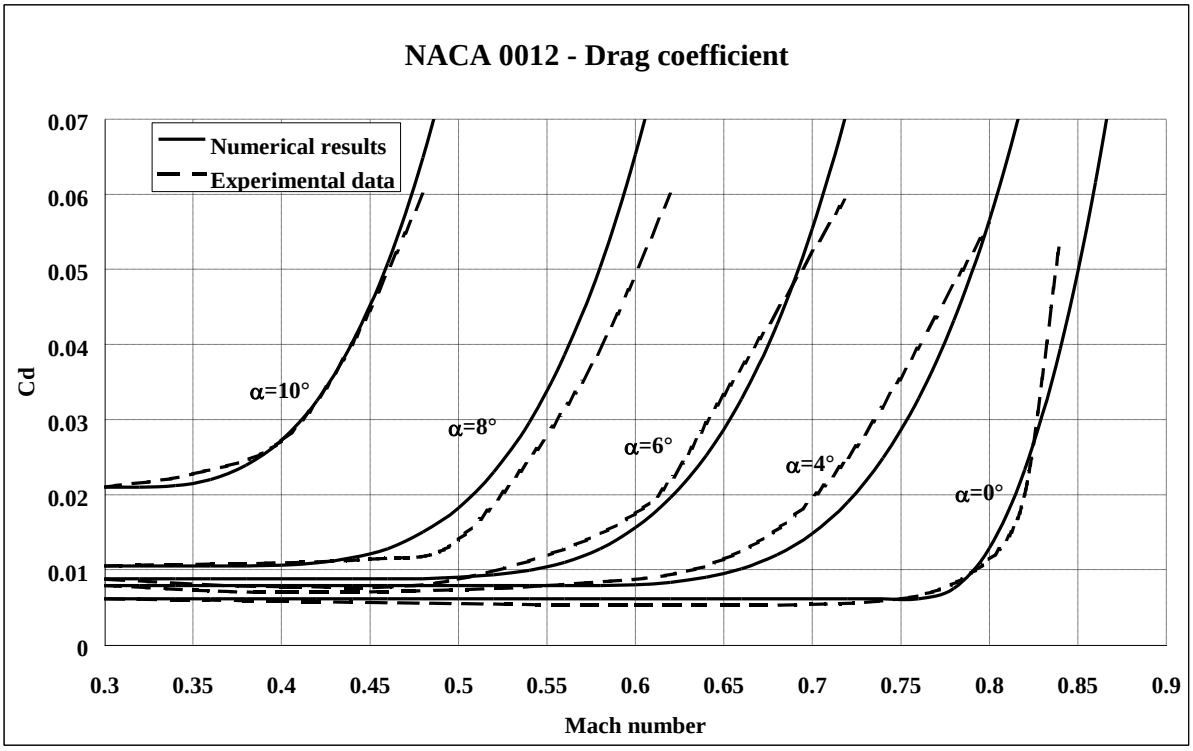

Fig. 4 – NACA 0012: Drag coefficient versus Mach number and angle of attack

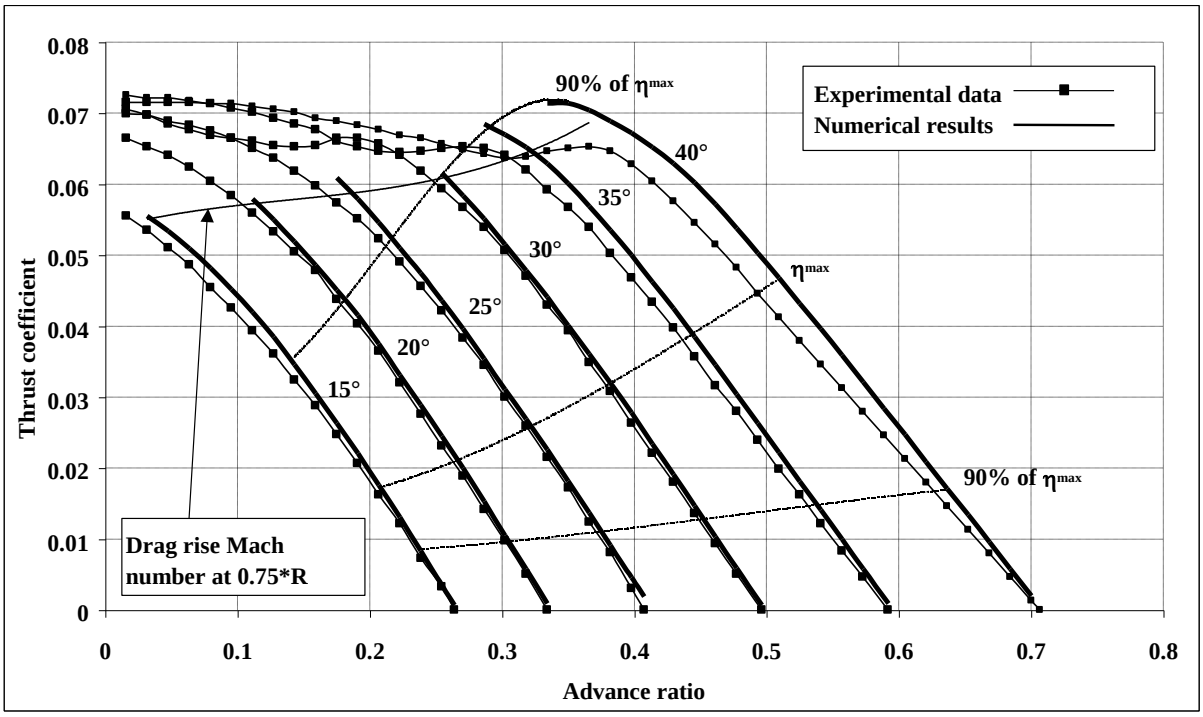

Fig. 5 – Thrust coefficient versus advance ratio and blade pitch angle

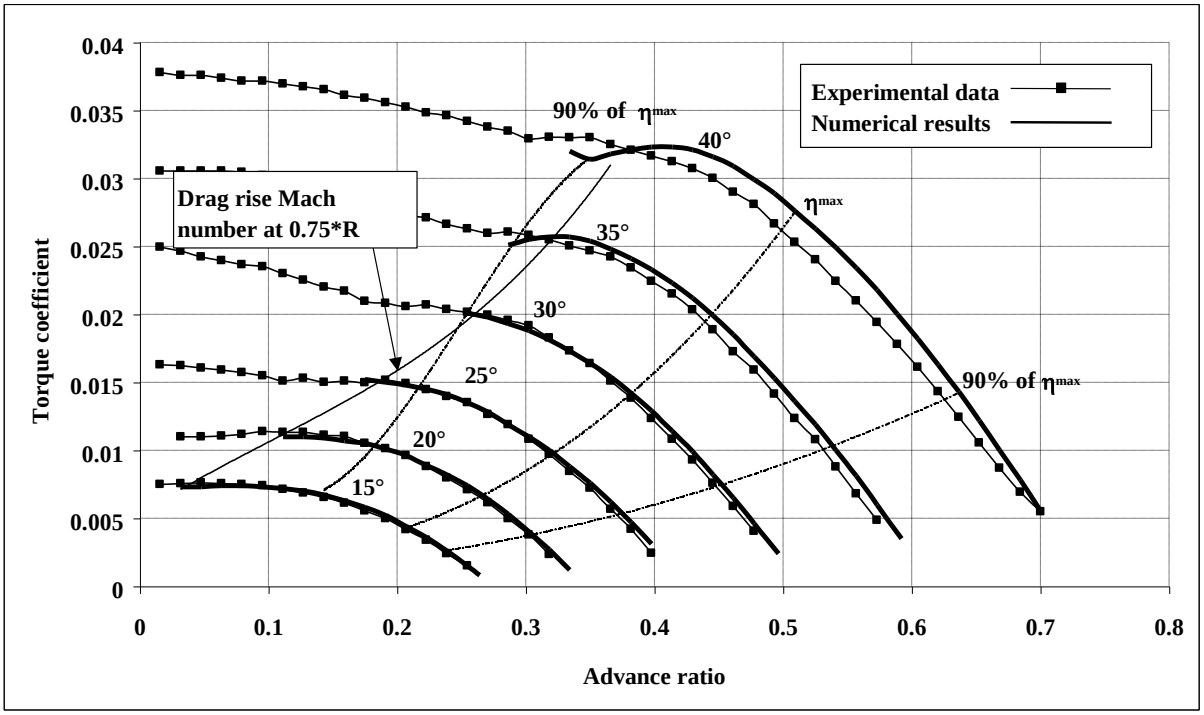

Fig. 6 – Torque coefficient versus advance ratio and blade pitch angle

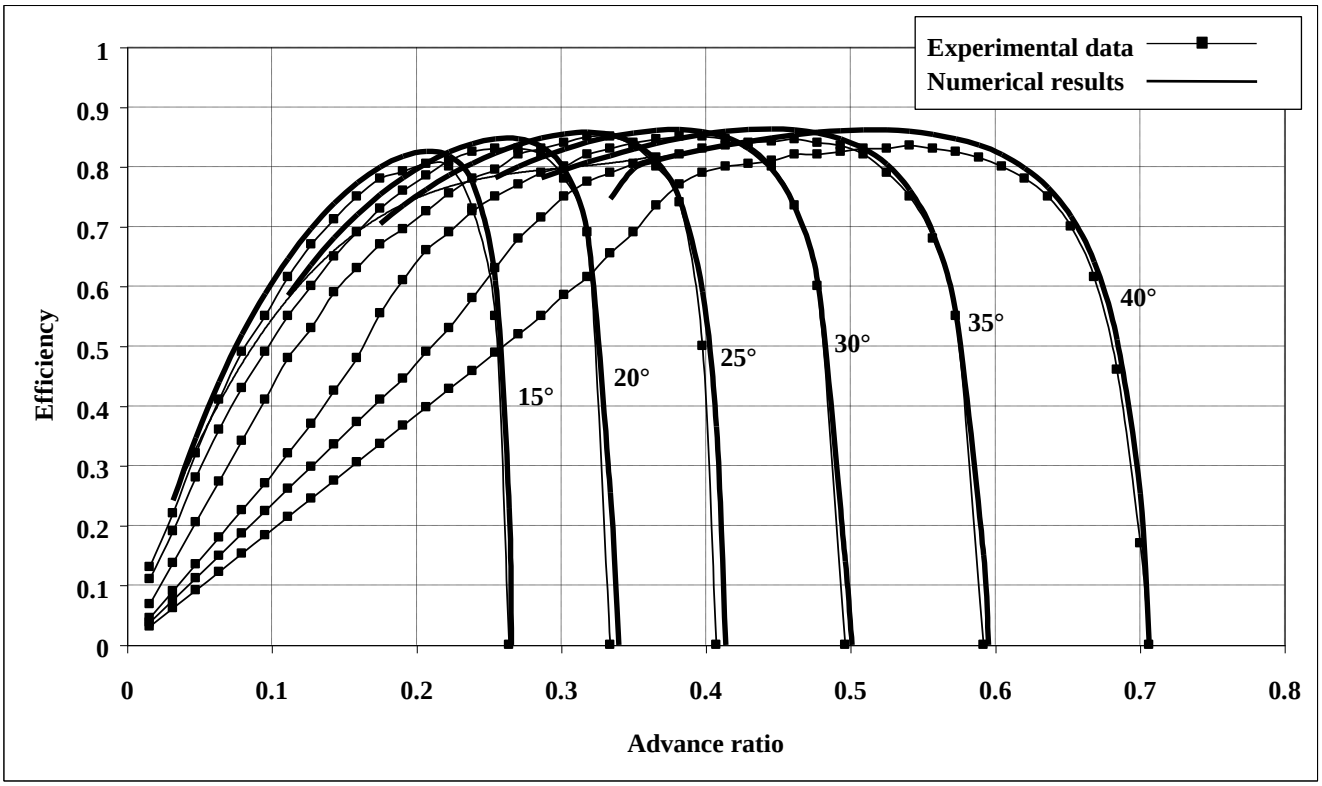

Fig. 7 – Efficiency versus advance ratio and blade pitch angle

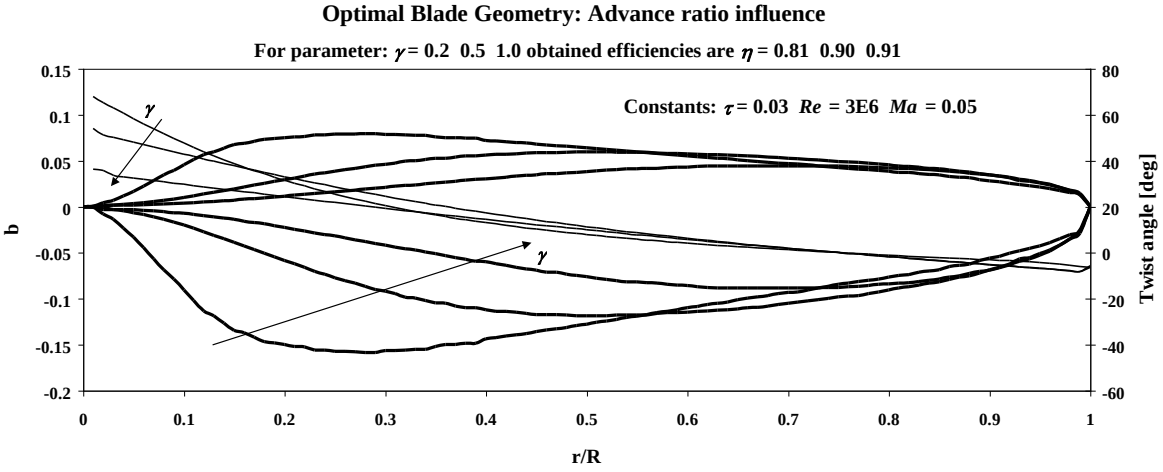

Fig. 8 – Advance ratio effects

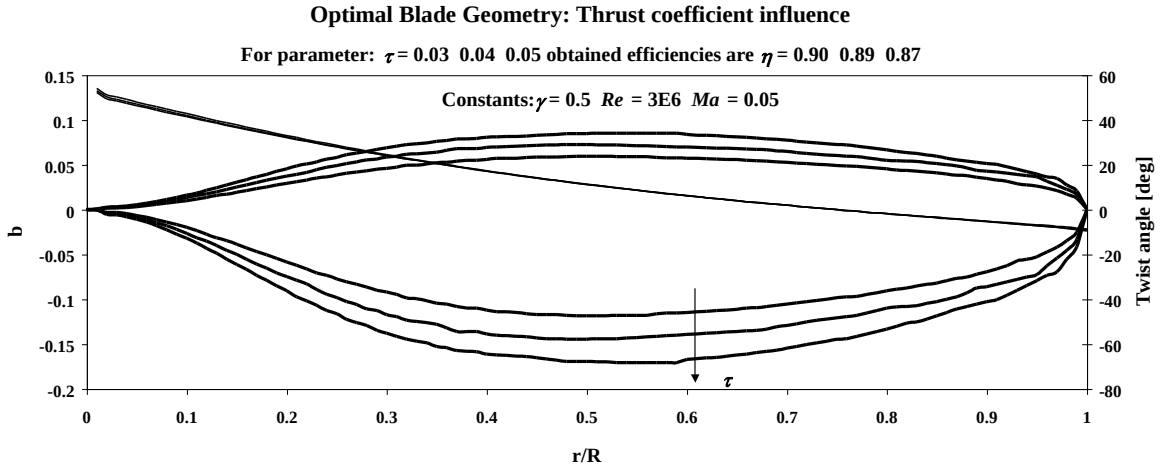

Fig. 9 – Thrust coefficient effects

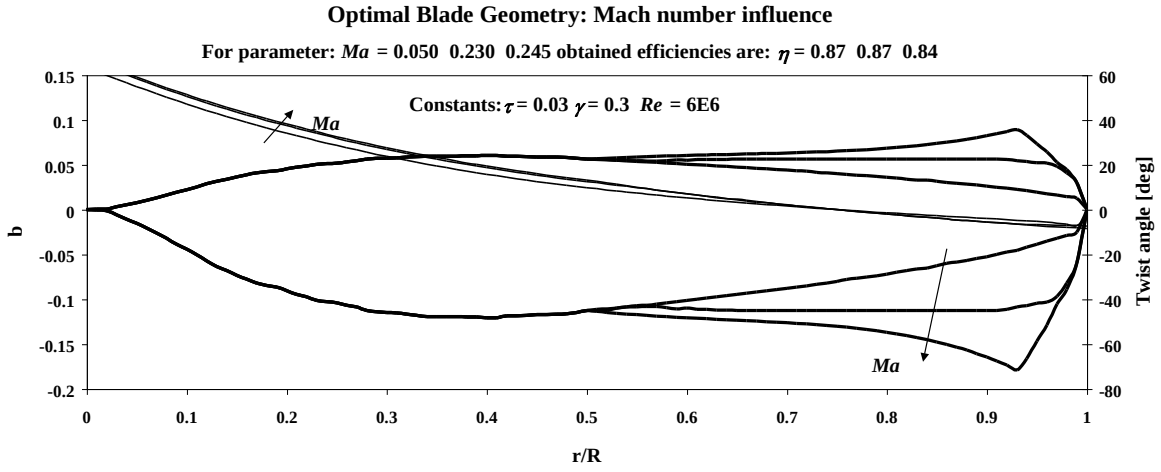

Fig. 10 – Mach number effects

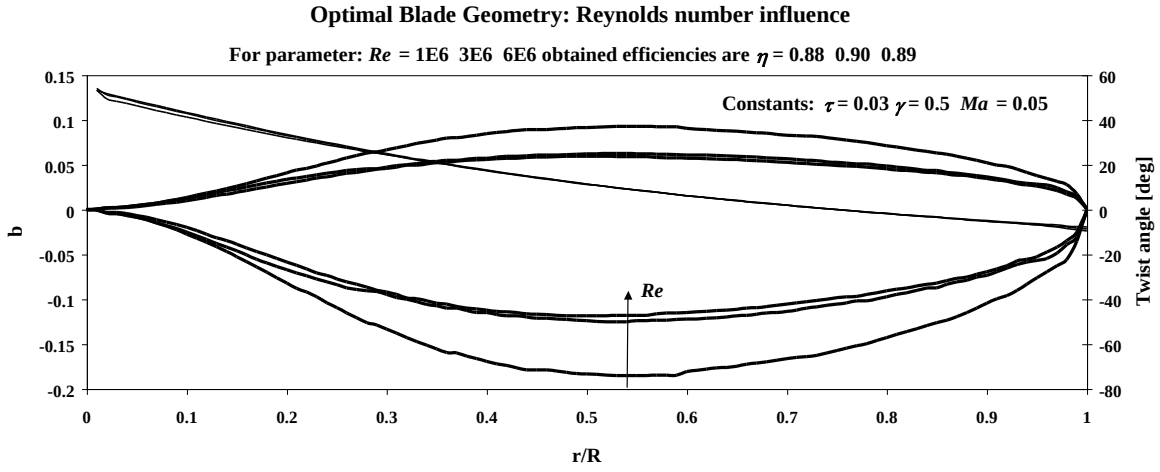

Fig. 11 – Reynolds number effects